nature physics

SUPPLEMENTARY INFORMATION

DOI: 10.1038/NPHYS2103

Stacking-dependent band gap and quantum transport in trilayer graphene

W. Bao[1], L. Jing[1], J. Velasco Jr. [1], Y. Lee[1], G. Liu[1†], D. Tran[1], B. Standley[2], M. Aykol[3], S. B. Cronin[3], D. Smirnov[4], M. Koshino[5], E. McCann[6], M. Bockrath[1,2], and C.N. Lau[1*]

[1] Department of Physics and Astronomy, University of California, Riverside, CA 92521

[2] Department of Applied Physics, California Institute of Technology, Pasadena, CA 91125

[3] Department of Electrical Engineering, University of Southern California, Los Angeles, CA 90089

[4] National High Magnetic Field Laboratory, Tallahassee, FL 32310

[5] Department of Physics, Tohoku University, Sendai, 980-8578, Japan

[6] Department of Physics, Lancaster University, Lancaster, LA1 4YB, United Kingdom

[†] Current address: Department of Chemistry and Biochemistry, University of California, Los Angeles, CA 90095.

*Email: lau@physics.ucr.edu

I. Sample fabrication

Trilayer graphene (TLG) sheets are obtained by mechanical exfoliation onto Si/SiO_2 substrates. They are first identified by color contrast in an optical microscope and confirmed by Raman spectroscopy. TLG devices are fabricated by evaporating metal electrodes through well-aligned shadow masks. Details of fabrication are described in ref. S1. The electrodes consist of 3 nm of Ti and 50 nm of Al. The trenches are 2-5 μm wide and ~250 nm deep. The degenerately doped Si substrates act as back gates. For typical suspended devices, the back gate coupling ratio is $\sim 2.5 \times 10^{10}$ $cm^{-2}V^{-1}$.

II. Current Annealing

As-fabricated suspended TLG devices often have low mobility values. To improve mobility, we current anneal the devices prior to transport measurements[2]. Such annealing is performed at 4 K in vacuum by slowly ramping up the applied voltage while monitoring the current. Typically, optimal annealing is reached when the measured current starts to saturate (Fig. S1); the applied voltage is then ramped down to zero. A representative saturation current is about 0.2mA/μm/layer for both Bernal (B) and rhombohedral (r) stacking suspended trilayer samples.

After current annealing, the devices exhibit much higher mobility, with the charge neutrality point shifting to almost zero. For r-TLG devices, the minimum conductivity decreases significantly with annealing (Fig. S2).

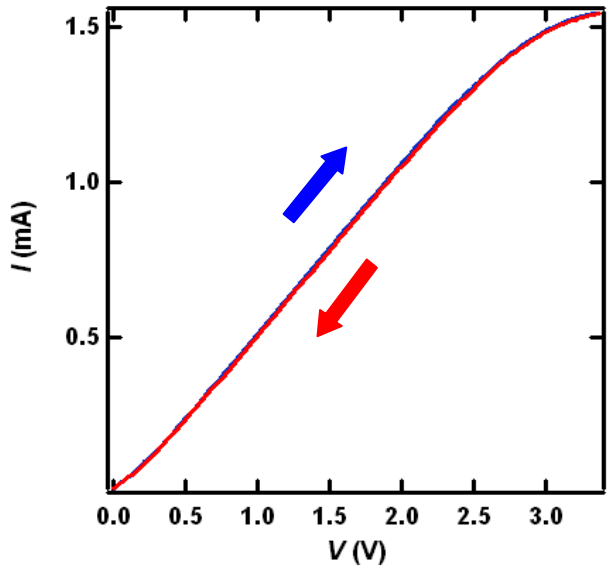

Figure S1. Current-voltage characteristics of a trilayer graphene device during current annealing. The arrows indicate voltage ramping direction. Optimal annealing is reached when current starts to saturate.

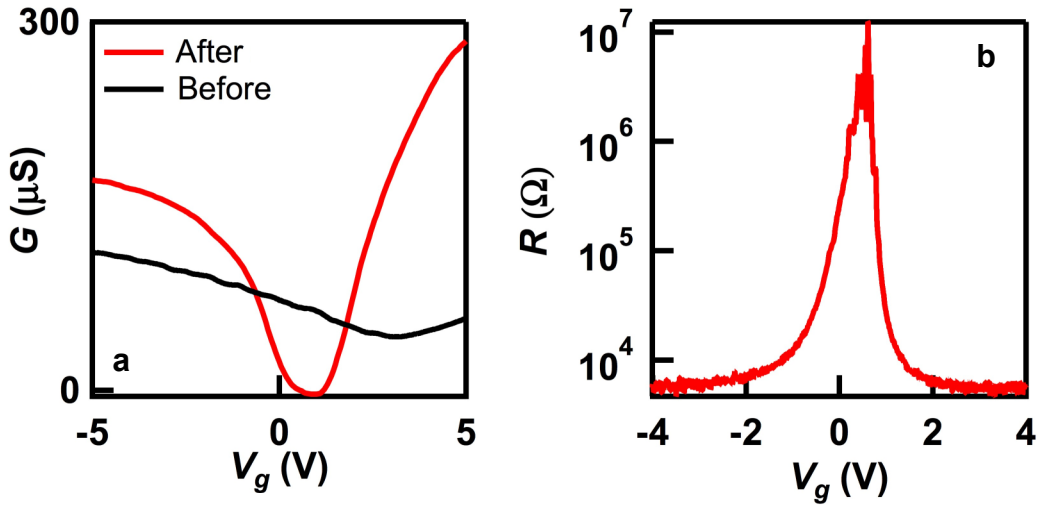

Figure S2. Transport data of an r-TLG device. a, $G(V_g)$ before and after annealing. **b,** $R(V_g)$ data of this device in logarithmic scale at T=1.5K. Note that R_{max}~10MΩ.

III. $G_{min}(T)$ of a Bernal-stacked TLG device

The conductance of suspended B-TLG devices has only moderate dependence on temperature. Fig. S3 displays the device conductance *vs.* gate voltage of such a device at temperatures between 4K and 300K. Its minimum conductance decreases by less than a factor of 2 over the entire temperature range. Generally the $G_{min}(T)$ curves cannot be satisfactorily accounted for by either thermally activated behavior or variable range hopping (Fig. S4).

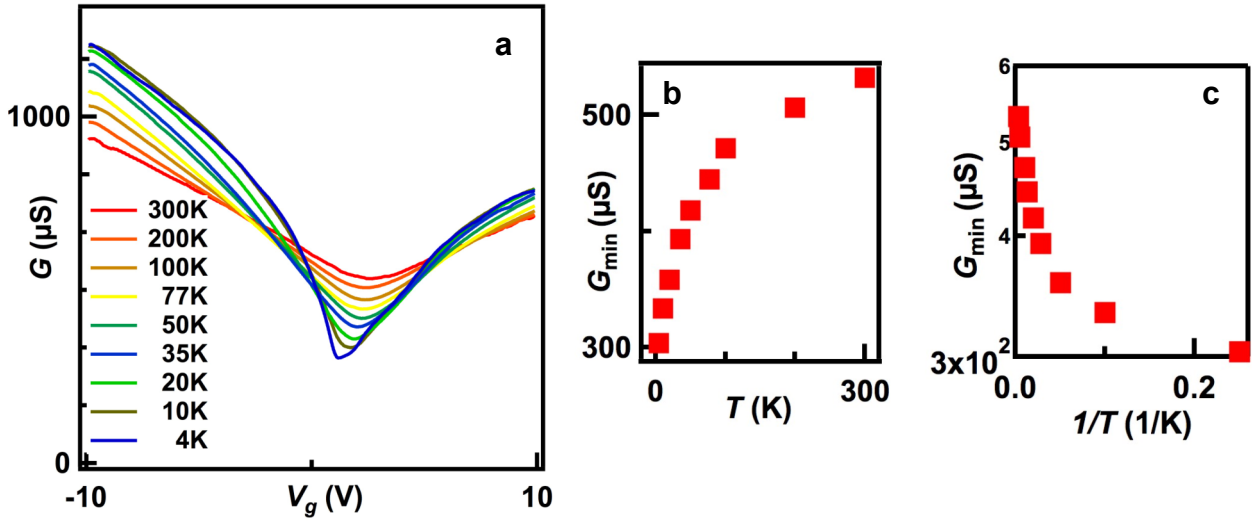

Figure S3. Temperature-dependent transport data of a B-TLG device. **a,** $G(V_g)$ of a suspended B-TLG device at different temperatures. **b-c,** G_{min} plotted *vs.* T and $1/T$, respectively.

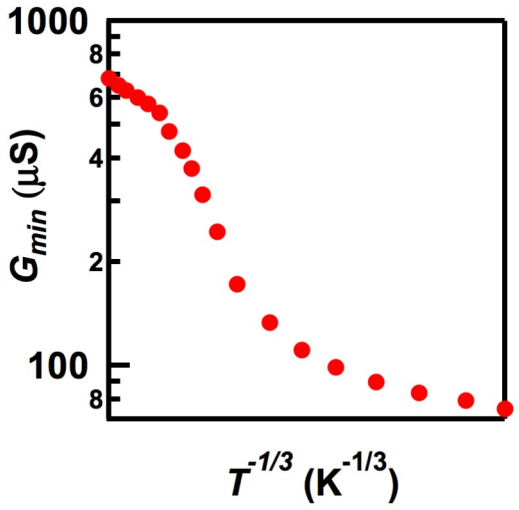

Fig. S4. The same data presented in Fig. 3c , plotted as G_{min} vs. $T^{-1/3}$.

IV. Role of Strains

Recent theoretical work[3] has suggested that strain could have a dramatic impact on the low-energy band structure of bilayer graphene. In the absence of strain and external fields, the low energy bands of bilayer graphene are described by a two-component effective Hamiltonian[4]:

$$H = -\frac{1}{2m}\begin{pmatrix} 0 & (\xi p_x - ip_y)^2 \\ (\xi p_x + ip_y)^2 & 0 \end{pmatrix} + v_3 \begin{pmatrix} 0 & \xi p_x + ip_y \\ \xi p_x - ip_y & 0 \end{pmatrix}, \qquad (1)$$

where $\boldsymbol{p}=(p_x,p_y)$ is in-plane momentum measured from the center of a valley, m is an effective mass, v_3 an effective velocity, and $\xi=\pm 1$ is a valley index. The first term dominates over a broad range of energy, yielding an approximately parabolic dispersion, while the second term is a source of trigonal warping that produces a distortion of the isoenergetic line away from a perfect circle. As the second term is linear in momentum, it has a dramatic effect at very low energy where there is a Lifshitz transition[4]: the isoenergetic line around each valley splits into four separate pockets, and this is reflected in the degeneracy of the low-lying Landau levels. The authors of Ref. 3 showed that homogeneous strain in bilayer graphene would produce an additional term in Eq.(1) that is independent of momentum. Thus, it has an important effect on the properties of low-energy bilayer graphene and the Lifshitz transition including, possibly, a dominance of $\nu=\pm 4$ states in the quantum Hall effect at low magnetic fields rather than $\nu=\pm 8$.

In contrast with the low-energy Hamiltonian of bilayer graphene Eq.(1), the low energy Hamiltonians of both B-TLG and r-TLG already contain terms that are independent of momentum even in the absence of strain. In B-TLG, such terms arise[5] from next-nearest-layer couplings γ_2 and γ_5, as well as the intrinsic energy difference between dimer and non-dimer sites (i.e. atomic sites with and without a partner atom directly above or below on the adjacent layer).

In r-TLG, such a term arises from next-nearest-layer coupling γ_2 [6,7]. The presence of these terms means that the role of strain will not be as dramatic on the low-energy trilayer band structure as it is in bilayers. Note, however, that the above discussion concerns homogeneous strain. Inhomogeneous strain could be relevant for both bilayers and trilayers, but we would expect its importance to vary from device to device depending on specific factors including geometry.

Moreover, we have studied a large number of devices with mobilities that span 3 orders of magnitude, and with different geometries and substrates (SiO_2 or the lack thereof). In all devices, r-TLG consistently displays much lower σ_{min} than B-TLG, and becomes insulating at the Dirac point for all suspended devices and 1 substrate-supported device (in contrast to the metallic behavior for all B-TLG devices). It is difficult to attribute such systematically different behaviours to strain or other extrinsic effects that are expected to display large sample-to-sample variations.

References

S1 Bao, W. Z. *et al.* Lithography-free fabrication of high quality substrate-supported and freestanding graphene devices. *Nano Research* **3**, 98-102 (2010).

S2 Moser, J., Barreiro, A. & Bachtold, A. Current-induced cleaning of graphene. *Applied Physics Letters* **91**, 163513 (2007).

S3 Mucha-Kruczynski, M., Aleiner, I. L. & Fal'ko, V. I. Band structure topology and Landau level spectrum for electrons in strained bilayer graphene. *preprint*, arXiv:1104.5029v1101 (2011).

S4 McCann, E. & Fal'ko, V. I. Landau-level degeneracy and quantum hall effect in a graphite bilayer. *Phys. Rev. Lett.* **96**, 086805 (2006).

S5 Koshino, M. & McCann, E. Gate-induced interlayer asymmetry in ABA-stacked trilayer graphene. *Phys. Rev. B* **79**, 125443 (2009).

S6 Koshino, M. & McCann, E. Trigonal warping and Berry's phase N pi in ABC-stacked multilayer graphene. *Phys. Rev. B* **80**, 165409 (2009).

S7 Zhang, F., Sahu, B., Min, H. K. & MacDonald, A. H. Band structure of ABC-stacked graphene trilayers. *Phys. Rev. B* **82**, 035409 (2010).